THE FEASIBILITY OF AN OPTICAL FLOW ALGORITHM FOR ESTIMATING ATMOSPHERIC MOTION

Wayne Bresky

Raytheon Information Solutions
Lanham, Maryland 20706

Jaime Daniels

NOAA/NESDIS
Center for Satellite Applications and Research
Camp Springs, Maryland 20746

ABSTRACT

Many operational algorithms to derive atmospheric motion vectors from satellite imagery utilize some form of pattern matching technique. Two of the more familiar techniques are the sum of squared differences and the cross correlation methods, both of which seek to find the maximum correlation between the initial target and subsequent match scene. In particular, the operational algorithm in use at NOAA/NESDIS minimizes the sum of squared differences while incorporating a forecast wind field to limit the size of the region being searched. In the field of computer vision one alternative to correlation-based tracking is the computation of the "optical flow" field. Methods to derive the optical flow field are fundamentally different from correlation methods in that the field of view or "neighborhood" is fixed in space while features move through the region. While an optical-flow based technique eliminates the need for a forecast wind field altogether, it does require that the displacements be relatively small so as to prevent the feature of interest from moving out of the field of view. For this reason, optical flow methods require high temporal resolution imagery to guarantee reliable results. This paper summarizes the experiences of the authors while testing one such optical flow algorithm. The algorithm tested here appears extensively in the computer vision literature where it is generally regarded as one of the more accurate approaches to estimate motion. In this paper we review the theory behind the selected optical flow technique before discussing modifications made for the current application. Following this discussion we present the results of testing done with a simulated (i.e., known) displacement and compare the optical flow field for this test case to the wind field derived using correlation-based tracking. This initial testing was vital to the refinement of the algorithm and proved that the optical flow method could be a viable alternative to the more traditional pattern-matching techniques. The rest of the paper is devoted to the application of the algorithm to real GOES water vapor data. The paper ends with a summary of our findings and a brief discussion of future avenues of research.

1. INTRODUCTION

Pattern matching techniques have been in use by the winds community since the advent of automatic tracking (Merrill, 1989). Two of the more familiar techniques are the cross-correlation and least-squares methods, both of which seek to find the best agreement between an initial target scene and a matching area found in a second image. At NESDIS a short-range (6-12 hour) forecast is used to estimate where to begin the search process before the algorithm computes the sum of squared differences for all possible scenes in the search array. The scene corresponding to the smallest sum is then selected as the match. This process is repeated forward and backward in time before a final average vector is computed from the two individual estimates.

In the field of computer vision pattern matching is just one of many techniques employed to estimate motion from a sequence of images. One alternative approach to correlation-based methods is the computation of the "optical flow" field (Horn and Schunk, 1981). In this approach, the target scene remains fixed in space as features translate through a field of view or "neighborhood." Changes in the brightness pattern are assumed to be the result of a simple translation of the brightness contours. Because the neighborhood is stationary a forecast wind field isn't required to guide the search process. On the other hand, optical flow techniques should not be used to estimate relatively large displacements as this suggests that the feature of interest has moved beyond the domain of the fixed neighborhood. These considerations imply that high temporal resolution imagery is required to achieve reliable results.

In this paper we test one such optical flow algorithm in an attempt to determine whether or not it may be used to estimate atmospheric motion from satellite imagery. In section 2 we discuss the general theory behind optical flow techniques before proceeding on to a discussion of the specific algorithm used in this application. In section 3 we present results from both the correlation-based and optical flow methods for a test case involving a known displacement. Testing the optical flow algorithm with a know displacement was crucial to validating the results and led to important refinements of the original algorithm. In section 4 we apply the optical flow algorithm to real GOES water vapor imagery and present some radiosonde match statistics to quantify the accuracy of the algorithm. The statistics are very encouraging, demonstrating a significant improvement in quality over the control, correlation-based result. We conclude the paper in section 5 by summarizing our findings and briefly discussing future avenues of development.

2. OPTICAL FLOW ALGORITHM

2.1. OVERVIEW

The field of computer vision defines the optical flow as the apparent motion of image brightness patterns in an image sequence. In the past 25 years or so numerous optical flow approaches have been documented in the literature (see Barron et al., 1994, for a comprehensive review). At the center of most optical flow algorithms is the so called *brightness constancy equation:*

$$\mathbf{V} \bullet \nabla I = -\frac{\partial I}{\partial t} \qquad (1)$$

Where I(x,y,t) is the image intensity and **V** is the horizontal wind vector.

By itself, this equation (a single equation in two unknowns) yields only the component of motion parallel to the brightness gradient vector (Horn and Schunk, 1981). It does not reveal the component of motion perpendicular to the brightness gradient vector. This situation is referred to in the field of computer vision as the *aperture problem*.

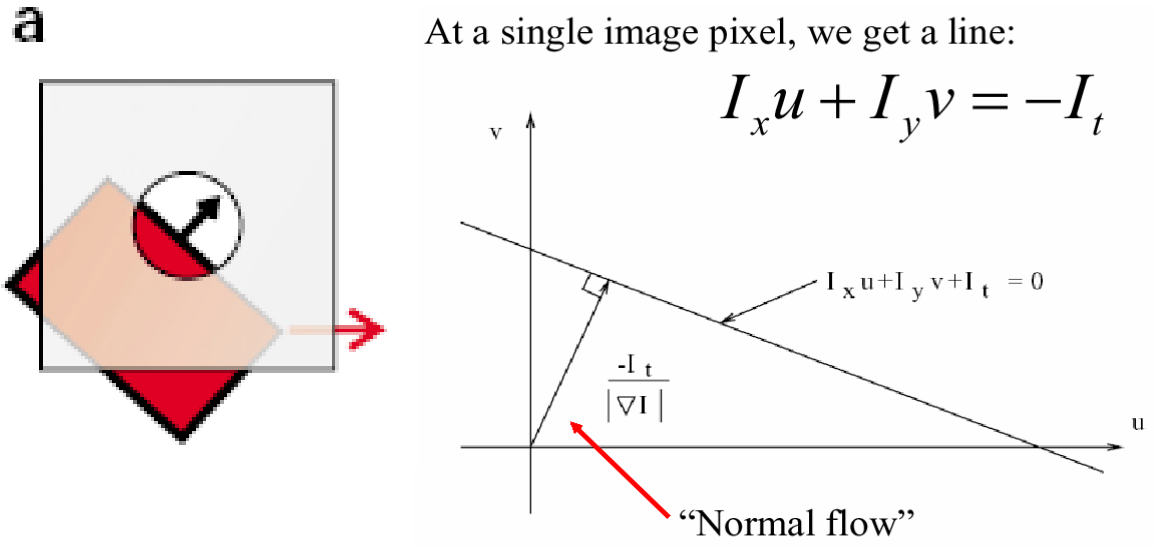

Figure 1. Aperture problem and normal flow. The picture on the left (a) depicts the aperture problem. The true motion of the red rectangle is towards the right (red arrow), but the velocity perceived through the small aperture is that shown by the black arrow. Only the component of motion parallel to the image gradient is determined. On the right, the brightness constancy equation describes a line in u- v- space that constrains the possible solutions. The solution depicted by the vector drawn from the origin (0,0) perpendicular to the constraint line is referred to as the "normal flow."

2.2 LUCAS-KANADE ALGORITHM

To circumvent the aperture problem Lucas and Kanade (1981) proposed that equation (1) be applied to a small neighborhood of pixels around the region of interest. In essence, the authors introduced the additional constraint that the velocity be constant over the neighborhood and then solved the resulting set of equations for the flow at the center of the neighborhood. They proposed solving the following system of linear equations

$$\underbrace{\begin{bmatrix} \nabla I(p_1) \\ \nabla I(p_2) \\ \vdots \\ \nabla I(p_{K^2}) \end{bmatrix}}_{\mathbf{A}} \underbrace{\begin{bmatrix} u \\ v \end{bmatrix}}_{\mathbf{d}} = - \underbrace{\begin{bmatrix} I_t(p_1) \\ I_t(p_2) \\ \vdots \\ I_t(p_{K^2}) \end{bmatrix}}_{\mathbf{b}}$$

where A is a matrix of spatial gradients, d is the displacement vector and b is a vector of temporal derivatives (also called response values). If the neighborhood is taken to be a K x K box then there will be K^2 linear equations. It follows that the solution is given by

$$\mathbf{d} = \left(A^T A\right)^{-1} A^T \mathbf{b}. \qquad (2)$$

The matrix to be inverted on the right hand side of equation (2) has been called the "structure" matrix (Trucco and Verri, 1998) because the eigenvalues of this matrix measure edge strength while the eigenvectors describe the edge direction. If the gradient vectors for an entire neighborhood all have the same direction (i.e., a single edge) then the minor eigenvalue vanishes and the system can not be solved directly.

2.2.1 IMPLEMENTATION

The over-determined set of equations resulting from (2) serves as the basis of the current algorithm. There are many ways to solve this system of equations. One way would be to solve it directly using Cramer's Rule (Fraleigh and Beauregard, 1987). This approach, however, fails if the structure matrix is singular, as noted above. To avoid this situation we choose instead to solve the system of equations using the method of Singular Value Decomposition (SVD, Press et al., 1986).

2.2.2 SMOOTHING

In the current application we start with a sequence of five images. Following the practice of many authors (Barron et al., 1994, Simoncelli et al., 1991) we begin by smoothing the imagery in both the spatial and temporal domains using a Gaussian filter. The spatial smoothing is performed first on all five images using a 2-D Gaussian filter with standard deviation of 3 pixels. This is followed by smoothing of the three middle images in the temporal domain using a 1-D Gaussian filter with standard deviation of 1 pixel-frame. The smoothing is done to remove noise in the imagery as well as in the computation of the derivatives.

2.2.3 TARGET SELECTION

The same target selection used by the operational winds algorithm was also used in this study. This was done to facilitate the comparison of the test winds with the control winds. By no means is this target selection an optimal approach when computing the optical flow. A selection method more suited to optical flow tracking might be to search the target image entirely and only track the strongest "corner" features (features with two strong edges).

3. SIMULATED 2-LINE/ELEMENT SHIFT

The optical flow algorithm outlined above was tested initially on a sequence of images with a known displacement. The starting point for the sequence was a single, full resolution, GOES-11 infrared image. This initial image was displaced by a known

amount (2-lines/elements) a total of four times to produce a sequence of five images, all exhibiting the same shift. The entire sequence was then smoothed spatially with a 2-D Gaussian filter before applying a 1-D Gaussian filter to the middle three images to achieve the temporal smoothing. A similar, but un-smoothed, test sequence was also created for the purpose of generating winds with the routine, correlation-based, algorithm. The results achieved with the test sequence are shown below in Figure 2.

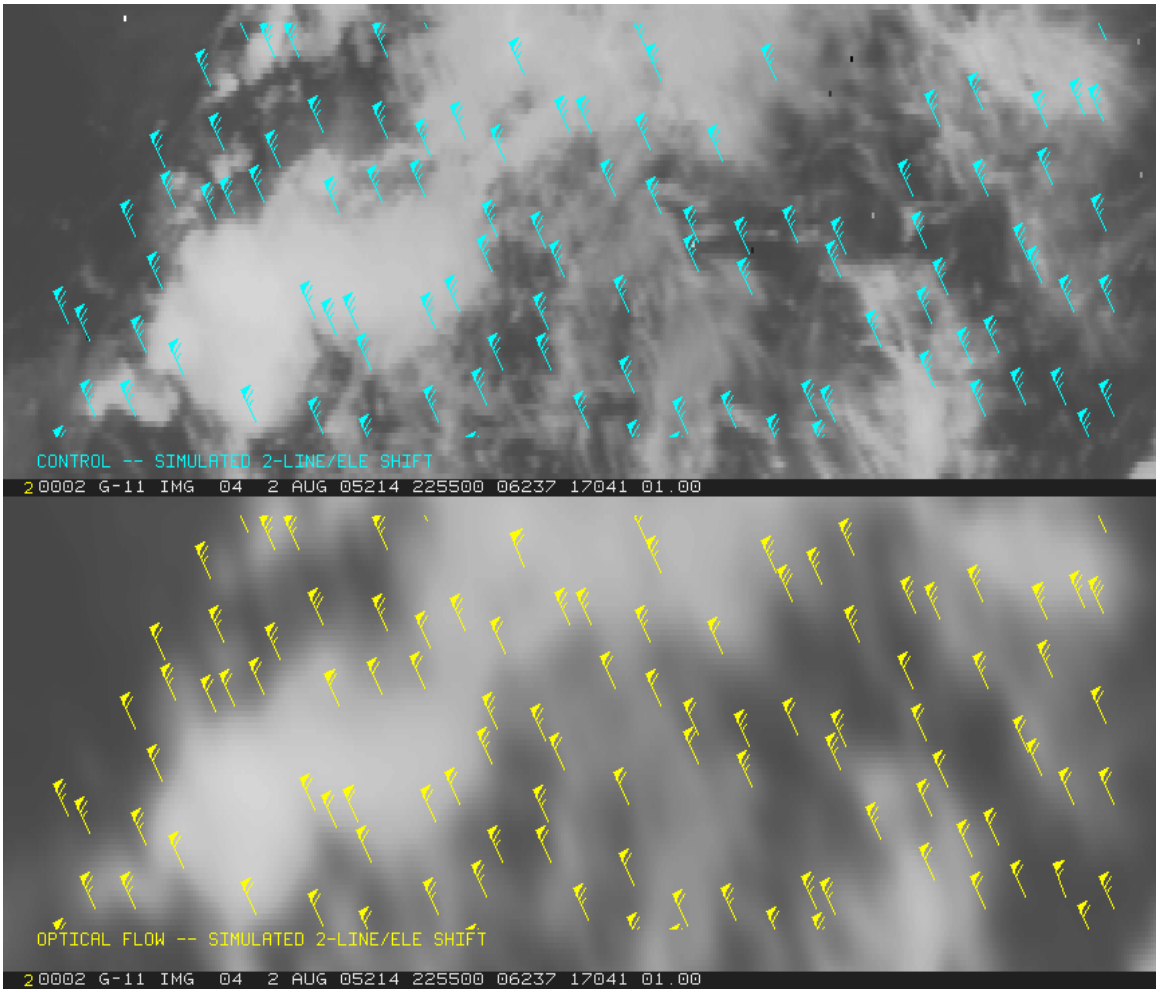

Figure 2. The control (top) and optical flow (bottom) winds generated using a test sequence with a known displacement (2-lines/elements).

The preceding results demonstrate that the optical flow algorithm is working as intended and is yielding results comparable to the routine tracking method, at least for this simple test sequence.

4. WATER VAPOR RESULTS

We now turn our attention to results obtained while using sequences of actual GOES water vapor imagery. Initial attempts at processing the brightness values with the optical flow algorithm yielded poor results in regions of very low contrast. Consequently, we

decided to process with the *raw satellite counts* (10-bit data) instead of the brightness values (8-bit data). The increased precision resulting from this logistical change resulted in a dramatic increase in coverage and coherency of the winds in these low contrast regions. The optical flow results shown in the following sections were all derived using the raw satellite counts.

4.1 GOES-11 5-MINUTE DATA

The first case we will show uses a sequence of 5-minute GOES-11 water vapor imagery taken on August 2, 2005. At this time the G-11 satellite had been taken out of storage temporarily and was being operated in a rapid scan test mode.

The five images comprising the loop were all smoothed according to the procedure outlined above. Moreover, a relatively large neighborhood of 25 x 25 pixels was used to "stabilize" the solution and prevent the central feature (in this case the maximum gradient) from exiting the neighborhood. Figure 4 shows a zoomed in portion of the domain for this case. In this region of relatively low contrast the optical flow method

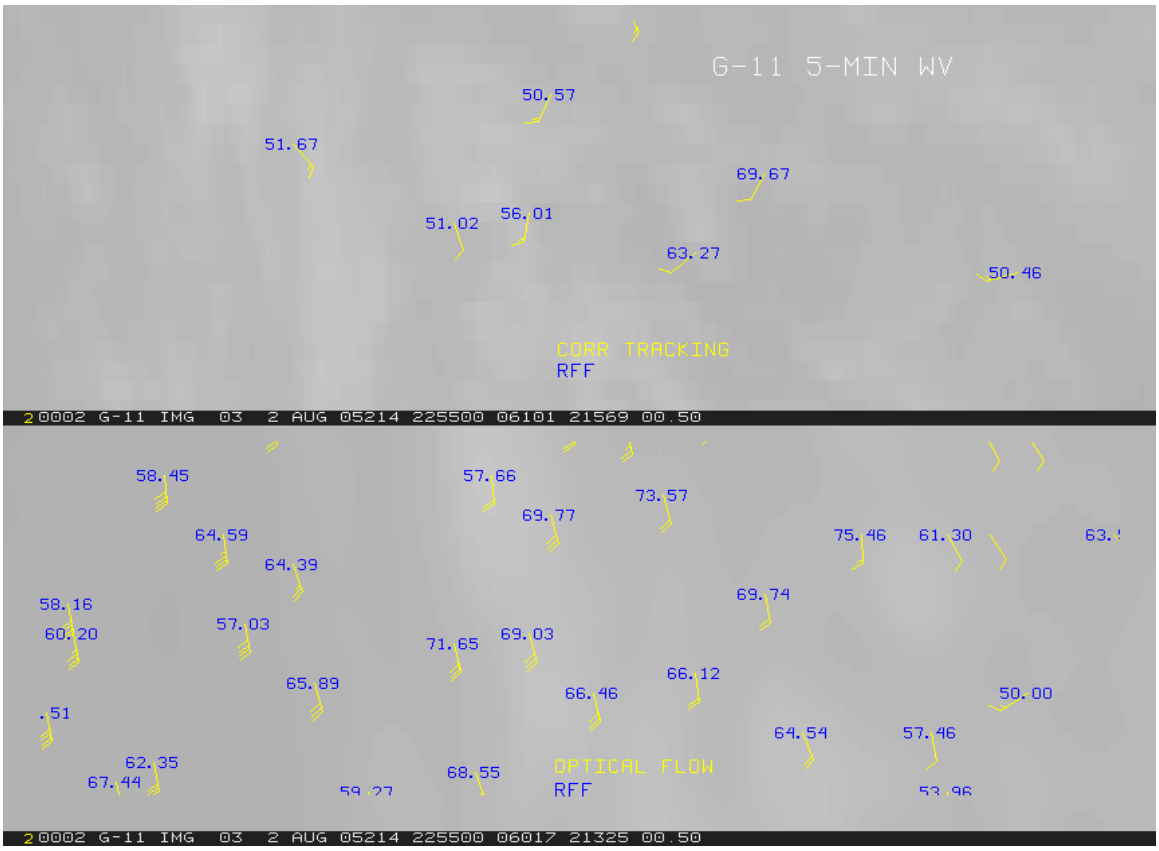

Figure 4. The routine (top) and optical flow (bottom) winds for 2255Z August 2, 2005. The recursive filter flag (RFF) value, an objective measure of quality, is shown in blue.

clearly seemed to outperform the routine tracking method, as evidenced by the higher RFF (an objective measure of quality based on an analysis of forecast and satellite data)

values in the bottom panel. Note also the much better coverage provided by the optical flow method.

In all fairness it should be noted that the routine correlation tracking for this case was performed using the brightness values and not the satellite counts, as was done with the optical flow test. This is because the operational winds software can only process 8-bit data. It is unclear how the routine algorithm would have performed with the increased precision afforded by the satellite counts.

4.2 G-12 RAPID SCAN DATA

The second example was generated using GOES-12 rapid scan (7.5 minute interval) imagery from April 3, 2006. The operational GOES satellites are frequently in Rapid Scan Operations (RSO) mode, particularly during severe weather outbreaks and when tropical cyclones threaten to make landfall in the US. As such, this case provides a more realistic scenario in which to evaluate the optical flow method in a "quasi-routine" setting. The optical flow winds for this case are shown below in Figure 5.

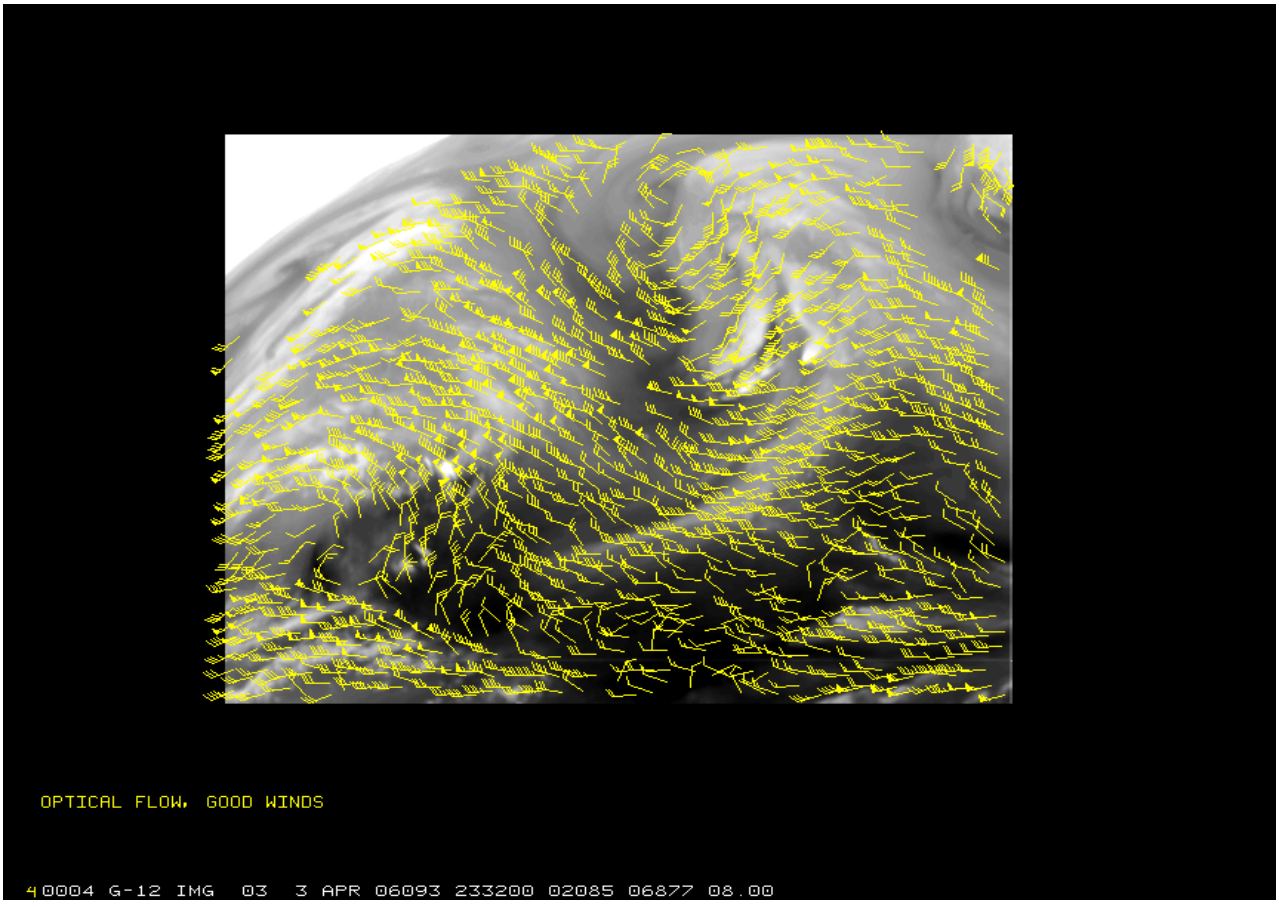

Figure 5. The water vapor winds for April 3, 2006 derived with the optical flow algorithm.

4.2.1 COMPARISON WITH RADIOSONDES

In order to assess quality, satellite winds are typically compared to collocated radiosonde or model forecast data. Here we chose to compare the winds to collocated radiosonde observations, mainly over the continental US (CONUS). Table 1 summarizes the results of our comparison of the clear-sky water vapor winds from this case.

Statistic	Correlation	Optical Flow
Mean Vector Difference	7.15	6.19
Normalized RMS	0.36	0.33
Sat-Raob Speed Bias	1.78	-0.57
Speed	23.82	20.85
Sample Size	160	160

Table 1. Comparison statistics between collocated GOES-12 edited water vapor winds (clear sky) generated using correlation matching and optical flow tracking and radiosondes at 00Z on April 4, 2006.

It is clear from this table that correlation tracking produces significantly faster winds than the optical flow estimate. This discrepancy might be the result of this method tracking small-scale features above the main water vapor layer. The smoothing process attendant with the optical flow approach may be removing these small-scale features while tracking the main layer further below. Whatever the cause, these statistics strongly suggest that the optical flow method is superior to the traditional correlation-based method for tracking clear-sky water vapor features.

5. CONCLUSIONS AND FUTURE PLANS

In this paper we tested an algorithm for computing the optical flow and evaluated its performance relative to a traditional pattern matching technique (sum of squared differences). The optical flow algorithm chosen for this paper is widely used in the field of computer vision, where it is regarded as one of the more reliable methods for estimating motion. The algorithm was tested initially on an image sequence with a controlled displacement to validate the results. Following this initial testing, we applied the new approach to actual GOES water vapor sequences and evaluated its performance relative to the correlation-based algorithm in current use at NESDIS. The evaluation included a comparison of the winds from both approaches to radiosonde wind observations. The results of the comparison suggest that the optical flow method is a useful, if not superior, alternative to correlation tracking. This is particularly true in regions of clear sky water vapor characterized by less structure.

On the other hand, the optical flow algorithm described here should not be used in jet regions with low temporal resolution imagery nor should it be used, in its current form, to track convective clouds. In the former situation the feature of interest is likely to move

beyond the boundary of the neighborhood, leading to an unreliable estimate. In the latter situation the brightness constancy assumption will clearly be violated. Given the relatively low (by computer vision standards) temporal resolution of today's operational satellites, the optical flow approach should probably be viewed as a replacement to correlation tracking only in certain limited situations.

Future work will focus on determining the largest allowable time interval that may be used with the optical flow algorithm. In addition, the algorithm will also be tested using data from other spectral bands (visible and infrared) to better define the conditions under which it will be of most use. Given what has been learned so far, and based on preliminary results (not shown) with infrared imagery, it appears the algorithm may be very useful for tracking low-level IR features. This will be explored more fully in future work.

Looking further into the future, plans are to relax the brightness constancy assumption by incorporating a more general constraint, such as the continuity equation, into the algorithm. There is also the possibility of relaxing the constant velocity assumption and allowing the flow to vary within the neighborhood by modeling the flow with an affine transformation.

REFERENCES

Barron, J.L., Fleet, D.J., Beauchemin, S.S., 1994. Performance of Optical Flow Techniques, *Int. Journal of Computer Vision*, **12**: 43-77.

Fraleigh, J.B., and Beauregard, R.A., 1987. *Linear Algebra*, Addison-Wesley.

Horn, B.K.P., and Schunck, B.G., 1981. Determining Optical Flow, *Artificial Intelligence*, **17**: 185-204.

Lucas, B.D., and Kanade, T., 1981. An Iterative Image Registration Technique with an Application to Stereo Vision, *Proc. 7th Int. Joint Conf. Artificial Intelligence*, 674-679.

Merrill, R., 1989. Advances in the Automated Production of Wind Estimates From Geostationary Satellite Imagery, *Fourth Conf. Sat. Met.*, 246-249.

Press, W.H., Flannery, B.P., Teukolsky, S.A., Vetterling, W.T., 1986. *Numerical Recipes*, Cambridge University Press.

Simoncelli, E.P., Adelson, E.H., and Heeger, D.J., 1991. Probability Distributions of Optical Flow, *Proc. Conf. Comput. Vis. Patt. Recog.*, 310-315.

Trucco, E., and Verri, A., 1998. *Introductory Techniques for 3-D Computer Vision*. Prentice Hall.